D19

A COMPUTATIONAL MODEL FOR A REGENERATOR

John Gary
Scientific Computing Division

David E. Daney
Ray Radebaugh

Chemical Engineering Science Division
National Bureau of Standards
Boulder, Colorado 80303

This paper concerns a numerical model of a regenerator running at very low temperatures. The model consists of the usual three equations for a compressible fluid with an additional equation for a "matrix temperature." The main difficulty with the model is the very low Mach number (approximately 1.E-3). The divergence of the velocity is not small, the pressure divergence is small, and the pressure fluctuation in time is not small. An asymptotic expansion based on the "bounded derivative" method of Kreiss is used to give a "reduced" model which eliminates acoustic waves. The velocity is then determined by a two-point boundary value problem which does not contain a time derivative. The solution obtained from the reduced system is compared with the numerical solution of the original system.

Key words: bounded derivative; compressible flow; cryocoolers; heat transfer; implicit scheme; numerical model; regenerator; stiff equations.

1. The differential equations

The oscillating flow takes place in a cylinder filled with small metal spheres [1]. The compressible flow equations are used to describe the flow around the spheres. A "resistance" term involving the resistance factor F is used to account for the porous media effects. The "matrix" of spheres has a heat capacity and heat can be transferred between the matrix and the gas. This conductance is determined by the coefficient h. The temperature of the matrix is given by T_m. The variables are listed in the appendix. The partial differential equations for these variables are the following.

$$\frac{\partial p}{\partial t} = -u\frac{\partial p}{\partial x} - \rho c^2 \frac{\partial u}{\partial x} + \frac{4G_r h}{D_h}(T_m - T) + \frac{2G_r F}{D_h}\rho|u|^3 \qquad (1)$$

$$\frac{\partial T}{\partial t} = -u\frac{\partial T}{\partial x} - G_r T \frac{\partial u}{\partial x} + \frac{4h}{C_v D_h}\frac{1}{\rho}(T_m - T) + \frac{2F}{C_v D_h}|u|^3 \qquad (2)$$

$$\frac{\partial u}{\partial t} = -u\frac{\partial u}{\partial x} - \frac{1}{\rho}\frac{\partial P}{\partial x} - \frac{2F}{D_h}u|u| \tag{3}$$

$$\frac{\partial T_m}{\partial t} = -\frac{4h\phi}{(1-\phi)\rho_m C_m D_h}(T_m - T) + \frac{\sigma}{\rho_m C_m}\frac{\partial^2 T_m}{\partial x^2} \tag{4}$$

The domain is $0 \leq x \leq L$. We will discuss the boundary and initial conditions in the next section. Their determination is crucial to the success of the numerical approximation.

To set up the numerical approximation we need to write these equations in dimensionless form. For this purpose we assume an ideal gas described by the following relations.

$$\rho = \frac{P}{R_c T} \qquad \rho c^2 = \frac{P}{\gamma} \qquad R_c = 2.03\ E{+}3\ J/kg{\cdot}K \qquad \gamma = 0.6$$

The scaling factors for the basic variables are the constants $(\bar{p}, \bar{u}, \bar{T})$. The time is scaled by the period (t) of the imposed oscillation in the mass flow. This is the same as the period of the piston oscillation. The x coordinate is scaled by the length L. We use $(\hat{p}, \hat{u}, \hat{T}, \hat{T}_m)$ for the scaled variables $(p/\bar{p},\ u/\bar{u},\ T/\Delta T,\ T_m/\Delta T)$.

$$\frac{\partial \hat{p}}{\partial t} = -\tau_1 \hat{u}\frac{\partial \hat{p}}{\partial x} - \frac{\tau 1}{\gamma}\hat{p}\frac{\partial \hat{u}}{\partial x} + \alpha_1 h\left(\hat{T}_m - \hat{T}\right) + \frac{\beta_1 \hat{p}\hat{F}}{\hat{T}}|\hat{u}|^3 \tag{5}$$

$$\frac{\partial \hat{T}}{\partial t} = -\tau_2 \hat{u}\frac{\partial \hat{T}}{\partial x} - G_r \tau_2 \hat{T}\frac{\partial \hat{u}}{\partial x} + \alpha_2 \frac{h}{\hat{p}}\left(\hat{T}_m - \hat{T}\right) + \beta_2 \hat{F}|\hat{u}|^3 \tag{6}$$

$$\frac{\partial \hat{u}}{\partial t} = -\tau_2 \hat{u}\frac{\partial \hat{u}}{\partial x} - \frac{1}{\epsilon}\frac{\hat{T}}{\rho}\frac{\partial \hat{p}}{\partial x} + \frac{1}{\epsilon}\frac{\beta_1}{G_r \tau_1}|u|u \tag{7}$$

$$\frac{\partial \hat{T}_m}{\partial t} = -\alpha_3 h\left(\hat{T}_m - \hat{T}\right) \tag{8}$$

Typical values of these dimensionless parameters are:

$\tau_1 = 0.92$	$\tau_2 = 14$	$\alpha_1 = 70$	$\alpha_2 = 709$
$\alpha_3 = 64$	$\beta_1 = 5.8E\text{-}4$	$\beta_2 = 8.7E\text{-}3$	$\varepsilon = 1.4E\text{-}5$

This is based on the values

$\bar{t} = 0.5$ s	$\bar{U} = 0.12$ m/s	$L = 0.057$ m	$R_c = 2.03E+3$ J/kg·K
$G_r = 0.65$	$C_v = 3.1E+3$ j/kg·K	$\bar{h} = 8.7E+3$ W/m^2·K	
$\bar{T} = 15$ K	$D_h = 1.2E\text{-}4$	$\bar{P} = 2$	

Clearly the term with the dominant coefficient is the one containing the factor ε^{-1}. The pressure must be very nearly constant in order to balance the terms in these equations. In order to avoid high velocity sound waves we must carefully set the initial and boundary conditions. The "bounded derivative" method of Kreiss is used to set the initial conditions. We chose the initial conditions so that the first two derivatives of the basic variables with respect to time are $O(1)$ rather than $O(\varepsilon^{-1})$. The work of Kreiss indicates that we can expect the time derivatives to remain bounded during the time integration of the partial differential equations. This implies that the fast sound waves do not appear, since their presence would require derivatives which are $O(\varepsilon^{-1})$.

2. The bounded derivative expansion

This method was developed by Kreiss [4]. Gustafsson has shown that, in certain cases, the results of Kreiss can be obtained by an asymptotic expansion [3]. Gustafsson has given a good expository treatment of the method [2]. If we assume an expansion of the basic variables in the form

$$\hat{p}(x,t) = \hat{p}_0(x,t) + \varepsilon \hat{p}_1(x,t) + \cdots$$

then we obtain a new system of equations for the functions (p_i, T_i, u_i, T_{mi}), $i = 0, 1, \ldots$ by equating like powers of ε in the usual way. Thus, we obtain from the velocity eq (7)

$$\frac{\partial \hat{p}_0}{\partial x} = 0.$$

The first term in the pressure expansion is therefore independent of x. Using this fact, eq (1) can be differentiated with respect to x to obtain an equation for the velocity (hereafter we drop the subscript "o" and the "^" modifier for the asymptotic expansion).

$$\frac{\partial}{\partial x}\left(\rho c^2 \frac{\partial u}{\partial x}\right) = \frac{\partial}{\partial x}\left[\frac{4hG_r}{D_h}(T_m - T) + \frac{2FG\rho|u|^3}{D_h}\right] \tag{9}$$

If the functions T and p are known and u is known at the boundary, then this equation can be solved for $u(x)$ in the interior. Equation (9) implies that the right side of the pressure eq (1) is independent of x. Therefore eq (1) can be regarded as an ordinary differential equation for $p(t)$.

Equation (2) can be regarded as a hyperbolic partial differential equation for $T(t,x)$ and eq (4) is an ordinary differential equation for $T_m(t,x)$. Note that these equations do not require any boundary conditions for the pressure p or the temperature T_m. If we regard the equation for the gas temperature as a hyperbolic equation, then we must specify T at an inflow boundary and leave it unspecified at an outflow boundary. We want to specify constant temperatures $T(t,o) = T_L$ and $T(t,L) = T_R$ at the boundary. However, when the flow reverses this would cause a discontinuity in the temperature at the boundary. Therefore we impose a fast exponential decay in time from the temperature at the time of reversal to the desired temperature T_L or T_R.

The velocity boundary values are chosen so that the mass flow is sinusoidal, that is

$$\rho(t,o)u(t,o) = C_o \sin(\omega t)$$

$$\rho(t,L)u(t,L) = C_L \sin(\omega t+\theta)$$

These conditions insure that mass is conserved over a cycle.

3. The numerical scheme for the asymptotic expansion

A finite difference mesh (t_n,x_i) is used where $t_n = n\Delta t$, and $x_i = iL/N$ for $0 \le i \le N$. The spatial derivatives are approximated by centered second order differences, for example

$$\frac{dT}{dX}(t_n,x_i) \cong \frac{T_{i+1}^n - T_{i-1}^n}{2\Delta x}$$

where T_i^n is the approximation for $T(t_n,x_i)$. An implicit type of predictor corrector is used which is similar to a Crank-Nicolson scheme. We will not write out the complete scheme for the full equations; instead we describe the scheme for the following simple equation

$$\frac{du}{dt} = u\frac{du}{dx}$$

Given the values at the nth time level, U_i^n, and an approximation $\hat{U}_i^o$ for U_i^{n+1}, then compute a corrected approximation $\hat{U}_i^1$ from

$$\frac{\hat{U}_i^1 - \hat{U}_i^n}{\Delta t} = \frac{\left(\hat{U}_i^o + U_i^n\right)}{2} \frac{\left(\hat{U}_{i+1}^1 + U_{i+1}^n - \hat{U}_{i-1}^1 - U_{i-1}^n\right)}{4\Delta x}$$

This is a tridiagonal linear system for the unknown vector $\hat{U}_i^1$. A correction is made for the variables p,T, and T_m in that order; then an updated value of the velocity is obtained by solving a finite difference version of eq (9) for U_i^n. If the heat transfer cofficient, h, is constant, then this is another tridiagonal linear system. If $h = h(u)$ depends on the velocity, then the resulting nonlinear equation is solved by a Newton iteration. The boundary conditions are described in the previous section. Generally, from two to five iterations (or corrections) were used. On the first iteration $\hat{U}_i^o = U_i^n$.

4. A fully implicit scheme for the original equations

We have a second computer code which is based on the original eqs (1) through (4) rather than the asymptotic expansion. Since $M_0^2 = \varepsilon$ is small we expect this sytem to be very stiff. Therefore, we expect that an implicit scheme is required. However, we use a CN (Crank-Nicolson) scheme rather than a BDF (backward-difference-formula). We choose the initial conditions to avoid the fast moving acoustic waves; therefore we do not need the BDF scheme to damp out the fast waves. We can choose arbitrary initial values for $T(x,o)$; however $p(x,o)$ is required to be constant and $u(x,o)$ must satisfy (9). This is the bounded derivative principle of Kreiss. The initial conditions are chosen so that the first two time deriatives of the solution (p, T, u, T_m) at $t = 0$ are bounded independent of ε.

The finite difference scheme uses three-point centered approximations for the spatial derivatives except at outflow boundaries, where a one-sided first order approximation is used. A Crank-Nicolson approximation is used in time. The difference scheme for each of the four variables is thus similar to (1) for the asymptotic approximation. However, the four equations are now coupled. Therefore, each time step requires the solution of a linear block-tridiagonal system with 4x4 blocks. We do not use a Newton iteration to deal with the nonlinearity. Instead, we use an iteration and evaluate the coefficients of the derivative terms at the previous iteration.

The boundary approximation for the temperature $T(x,t)$ is the same as for the asymptotic equations. The boundary conditions for $u(x,t)$ are specified at all times using the same values as in eq (6). There is no boundary condition for the p equation; instead one-sided differences are used to approximate derivatives at the boundary. No boundary condition is needed for the T_m equation since this equation contains no spatial derivatives.

5. Computational results

In this section we give some results obtained from the two numerical methods described in the previous sections. Unless otherwise stated, the results were obtained using the bounded derivative (i.e. asymptotic expansion) model. Within SI, many units choices exist for most quantities! In all of these runs the heat transfer coefficient between the gas and matrix was given by the term

$$h(m) = 40 \exp(-1.6m) + 220(1-\exp(-1.6m))m$$

where

$$m = \rho|u|.$$

The exponential factor is included to avoid a discontinuous derivative of $h(|\rho u|)$ with respect to to u at $u=0$.

The formula used to bring the boundary temperature of the gas back to its constant inflow value when the velocity reverses is

$$T(t) = T_L + \left(T_{rev} - T_L\right)\exp\left(\left(t_{rev}-t\right)/\tau\right)$$

Here T_L is the constant inflow temperature (15 K at the left boundary and 10 K at the right boundary for most of our runs) and T_{rev} is the temperature of the gas at the time when the velocity reverses direction. The time of reversal is t_{rev} and τ is an input parameter, whose value was 0.05P where P is the period of the mass flow oscillation.

The mass flow at the boundary is given by

$$\rho u = C \sin(2\pi ft+\theta)$$

where f is the frequency and θ is the phase. At the left boundary $\theta=0$, at the right values in the range $-45^{\circ}\leq\theta\leq 0^{\circ}$ were used.

All runs assumed an ideal gas with equation of state

$$p = Rc\ \rho T.$$

The specific heat of the gas at constant volume was

$$C_v = 3120.\ \ J/kg\cdot K$$

The thermal conductivity of the matrix was 0.3 W/m·K and of the gas was 0.13 W/m·K. The regenerator length was 0.0572 m.

5.1 The temperature and pressure wave forms

The temperature as a function of time at the left and right boundaries is given in figures 1 and 2. In this case, which we refer to as case I, the inflow temperatures at these boundaries were 15 K and 10 K; the mass flow amplitude was 77.9 kg/m^{2}s; the starting pressure was 3.3 Mpa; the heat capacity of the matrix was 2.64E+5; the hydraulic diameter was 1.21E-4; and the frequency was 5 Hz. The time interval shown is $12\leq t\leq 13$, that is, the system has been run for 60 cycles before these curves are drawn. The matrix temperature is shown as a dashed line; the gas temperature is a solid line. In this case, the two temperatures were almost identical. The temperature at a point 4/5 of the distance across the regenerator (x=0.8) is shown in figure 3.

The temperature as a function of position x across the regenerator at certain times in the cycle is shown in figure 4. The pressure oscillation is shown in figure 5.

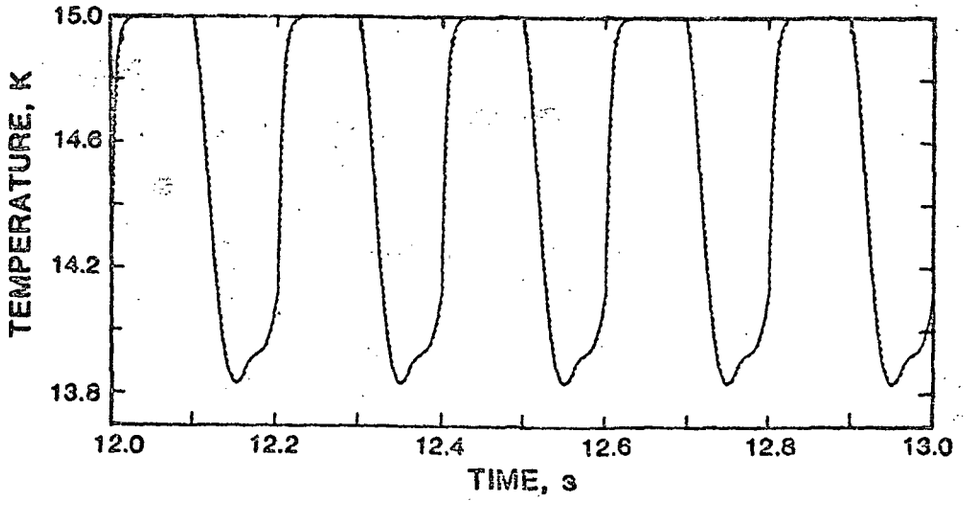

Figure 1. Temperature (K) vs. time (a) at x = 0 for case I.

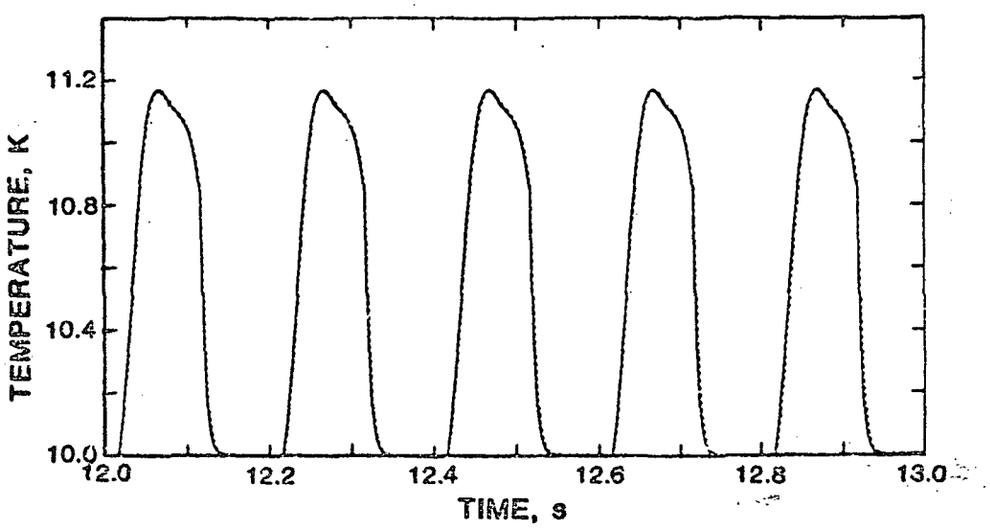

Figure 2. Temperature vs. time at x = 1.0 for case I.

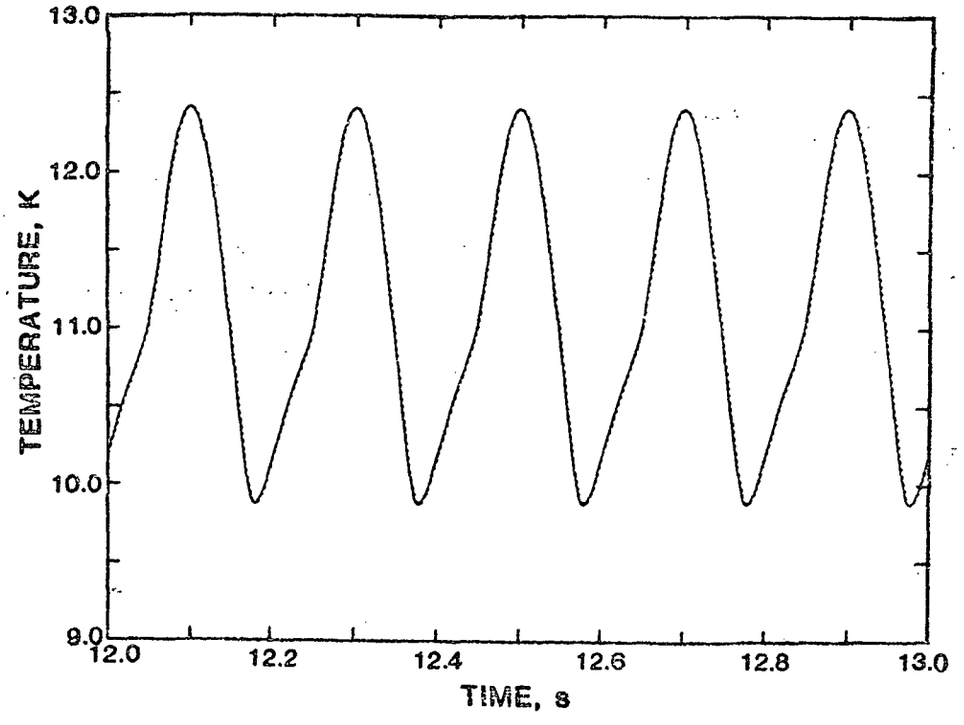

Figure 3. Temperature vs. time at x = 0.8 for case I.

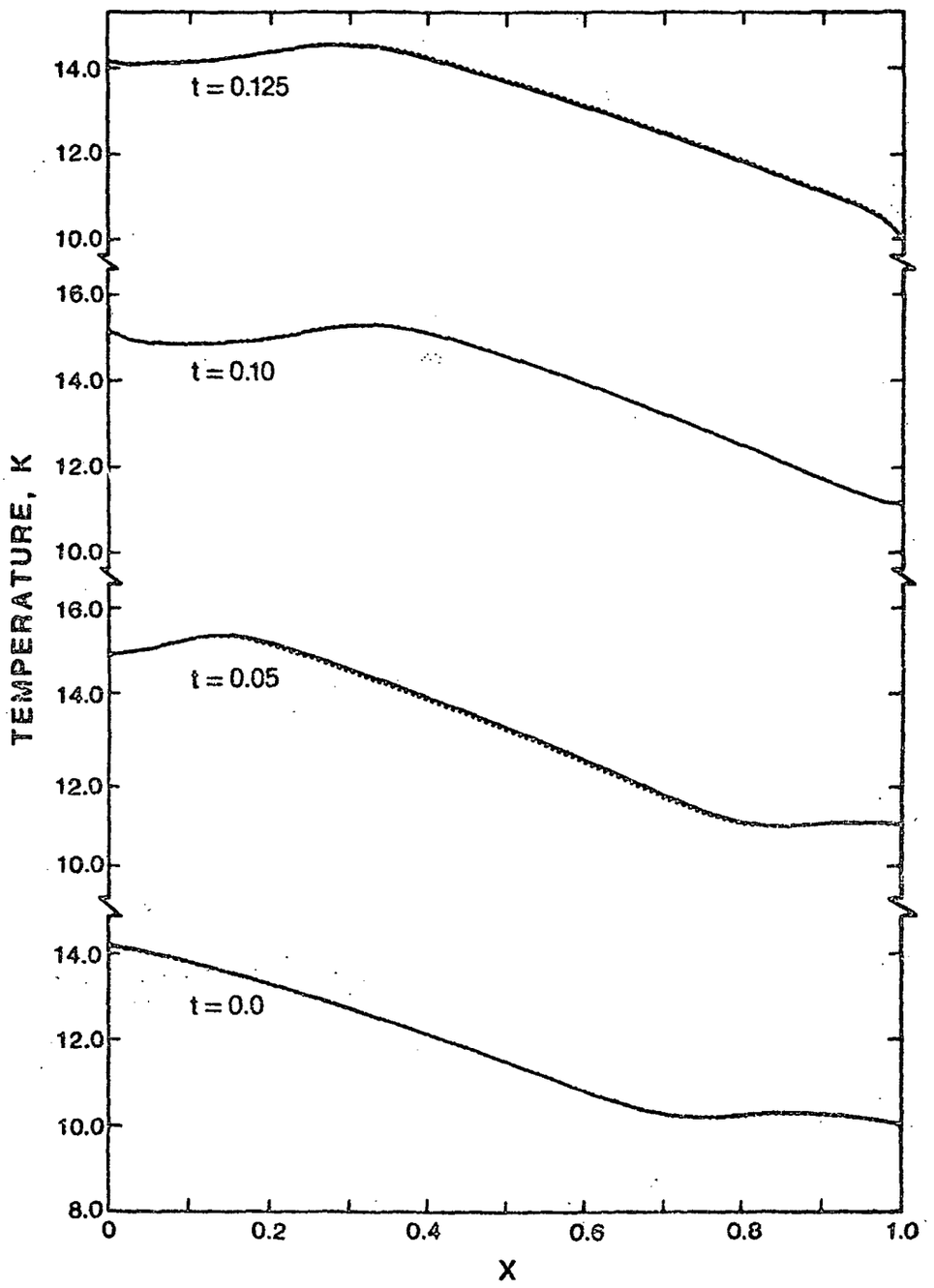

Figure 4. Temperature vs. x at the given t for case I.

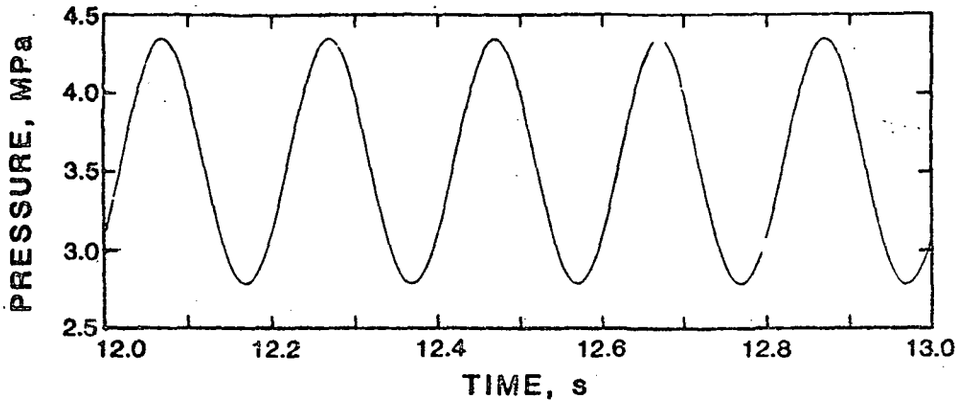

Figure 5. Pressure vs. time for case I.

5.2 The effect of the hydraulic diameter and matrix heat capacity

In figure 6 the temperature wave at the right boundary is shown. All parameters are the same as in case I above, except the hydraulic diameter has been increased by a factor of four. There is

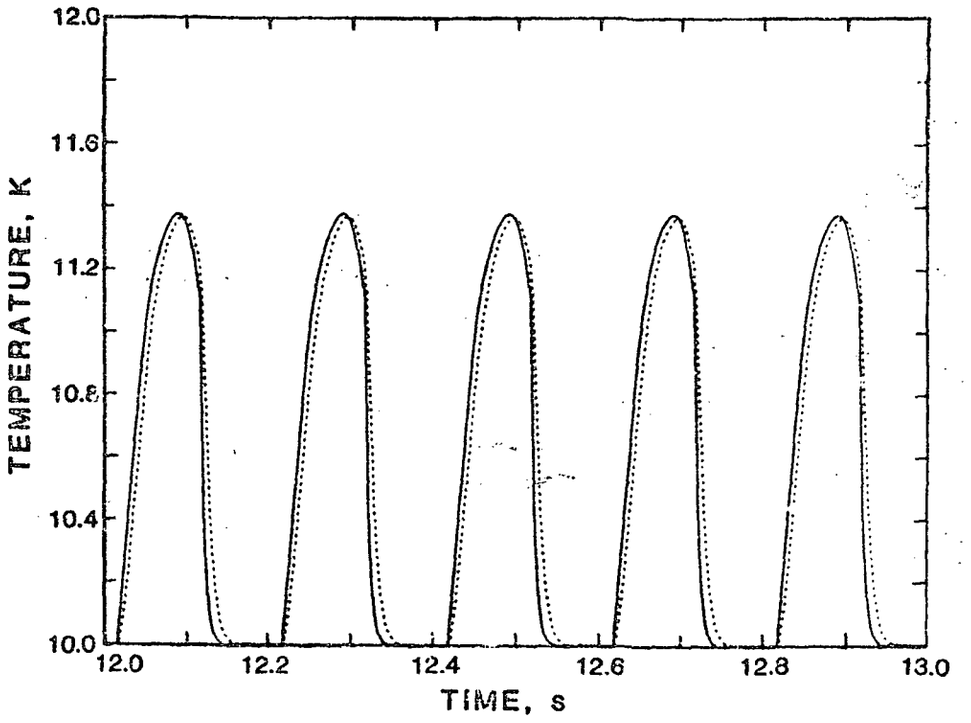

Figure 6. Temperature vs. time at x = 1.0 with D_h (hydraulic diameter) = 4.84E-4 m.

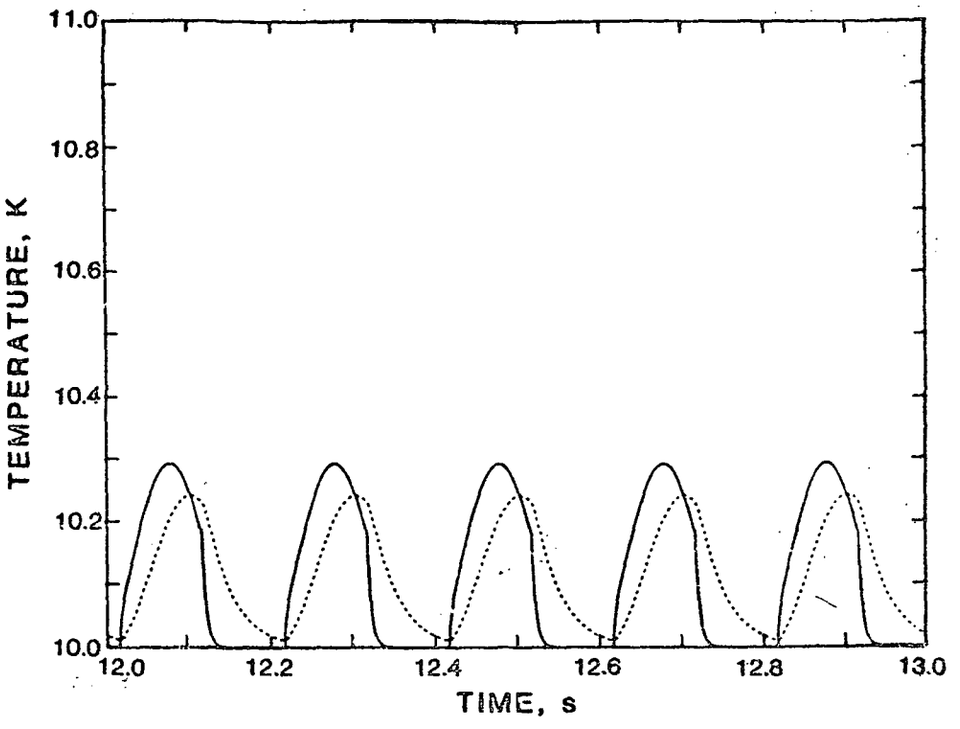

Figure 7. Temperature vs. time at x = 1.0 with $\rho_m C_m$ = 5.28E+6 J/kg·m^3.

now some separation of the matrix and gas temperature. A greater separation is seen in figure 7. Here the heat capacity of the matrix has been increased by a factor of 20 over case I.

Our definition of the ineffectiveness is given by the following integral which is taken over the outflow portion of the cycle,

$$\int \rho |u| (T(L,t)-T_L)dt \; / \; \int \rho |u| (T_o-T_L)dt.$$

Here T_o and T_L denote the fixed gas temperature and T(L,t) denotes the gas temperature o outflow. The ineffectiveness as a function of hydraulic diameter, D_h, is shown in figure 8 for the conditions of case I. In figure 9 the variation with matrix heat capacity, $\rho_m C_m$, is shown.

In table 1, we compare our computed ineffectiveness with that obtained by Daney using a model which assumes no pressure variation. Our results are higher, which is probably explained by our non-zero pressure swing during the cycle. The table shows that ineffectiveness increases with the pressure swing.

5.3 The accuracy and consistency of the model

In table 2 the value of the ineffectiveness is shown as a function of the numerical resolution. These results are for case I where the frequency is 5 Hz. Note that with Δt = 0.001 s and Δx = 0.1 we have 10 mesh intervals across the regenerator and 200 time steps per cycle. The last run with Δt = 0.004 s did not yield valid results. The need for a small time step may be explained by the rapid change in the temperature at the boundary. When the flow changes from outflow to inflow the temperature is raised to the boundary value in about 0.01 seconds in this case. Therefore we might expect some trouble with the larger time step.

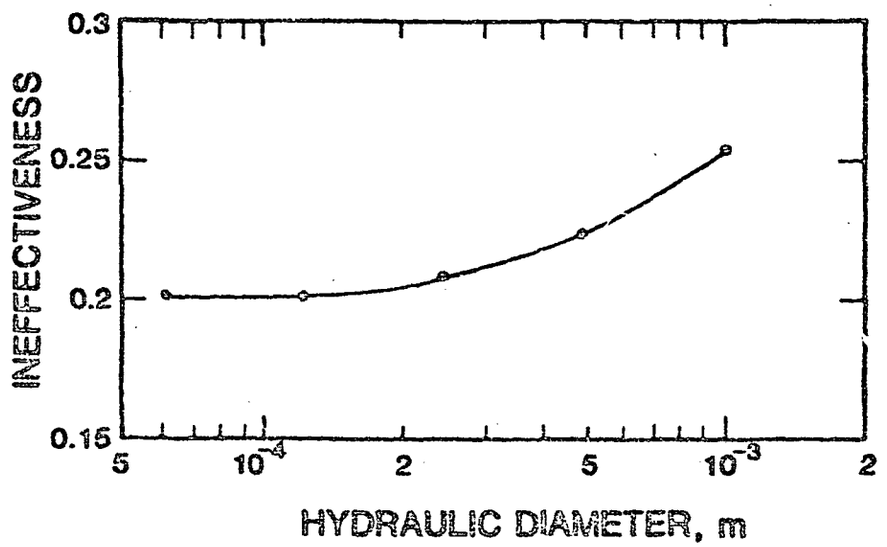

Figure 8. Ineffectiveness vs. hydraulic diameter.

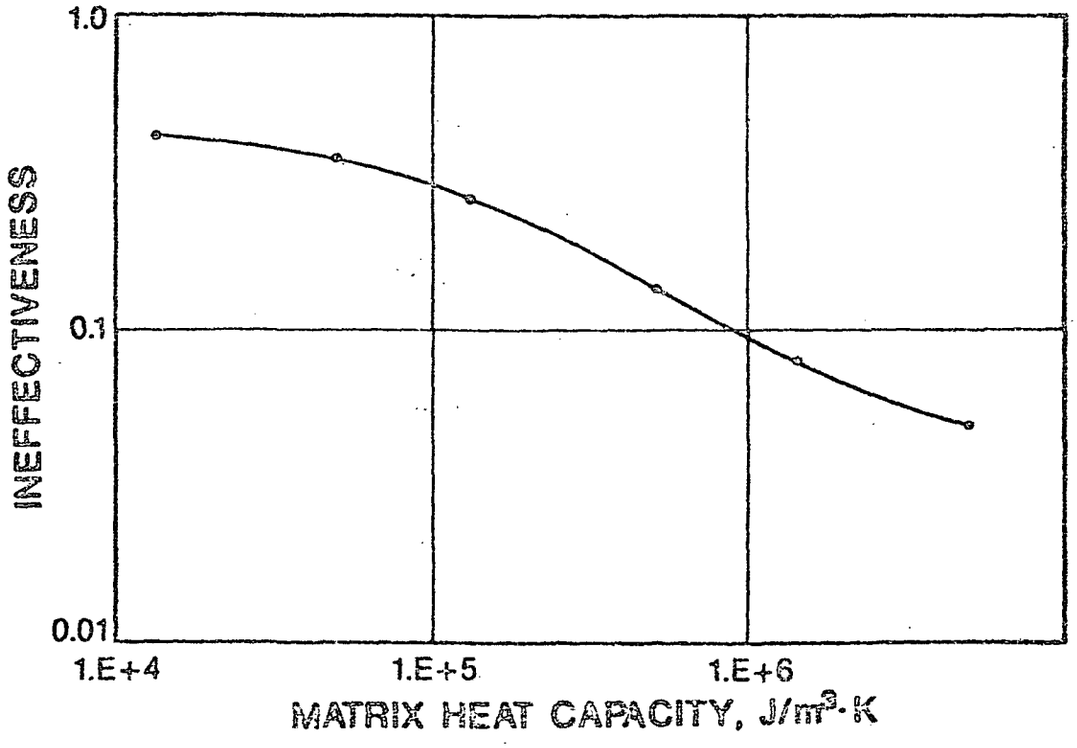

Figure 9. Ineffectiveness vs. matrix heat capacity.

Table 1. Comparison with Constant Pressure Model.

Model	Ineffectiveness	Temperature Swing K	Pressure Swing MPa
constant pressure (Daney)	0.015	—	
phase = 0.0	0.027	10.0 - 10.50	2.9 - 3.3
phase = -14°	0.079	10.0 - 10.62	2.8 - 3.8
phase = -29°	0.122	10.0 - 10.79	2.6 - 4.5

Table 2. Accuracy.

Resolution	Ineffectiveness
Δt = 0.001 s Δx = 0.1	0.207
Δt = 0.001 s Δx = 0.05	0.202
Δt = 0.0005 s Δx = 0.025	0.201
Δt = 0.004 s Δx = 0.05	0.23*

*Did not reach a steady state - mass loss 1% per cycle.

In table 3 we compare the results for case I obtained from the two models. The full equation solution shows a small oscillation in the velocity field which is not present in the solution using the reduced equations. The CPU time is on a CDC Cyber 750. The results for the two models seem to be in good agreement.

5.4 Achieving a quasi-steady state

The results described above were obtained by running the model for 66 cycles. At this point there is very little change of average or maximum values from one cycle to the next. For example, in case I the maximum gas temperature at the cold end is changing at a rate of 10^{-4} K per cycle. This is a very small change; however, this rate appears to be virtually constant over the last 10 or 20 cycles. Therefore, we don't know how close we are to a steady oscillation. At this rate 1000 cycles would be required to effect a 10 percent change in this maximum temperature. We need to find a method to accelerate convergence.

Table 3. Comparison of Reduced and Full Equations Models.

Model	Ineffectiveness	Temperature Swing K	Pressure Swing MPa	CPU Time/Cycle s
Reduced	0.202	10.0 - 11.2	2.7 - 4.3	6.8
Full	0.186	10.0 - 11.1	2.8 - 4.3	23

6. References

[1] Daney, D. and Radebaugh, R., Nonideal Regenerator Performance - the Effect of Void Volume Fluid Heat Capacity, Cryogenics 24, 499-501 (1984).

[2] Gustafsson, B., Numerical Solution of Hyperbolic Systems with Different Time Scales Using Asymptotic Expansions, Jour. Comp. Phys. 36, 209-235 (1980).

[3] Gustafsson B. Asymptotic Expansions for Hyperbolic Problems with Different Time-Scales, 17, 623-634 (1980).

[4] Kreiss, H., Problems with Different Time Scales for Partial Differential Equations, Comm. Pure. App. Math, XXXIII, 399-439 (1980).

Notation			SI Units
P	-	pressure	MPa
ρ	-	gas density	Kg/m^3
ρ_m	-	matrix density	kg/m^3
c	-	acoustic velocity	m/s
u	-	velocity	m/s
G_r	-	Grueneisen parameter	
h	-	heat transfer coefficient	$W/m^2 \cdot K$
D_h	-	hydraulic diameter	m
T	-	gas temperature	k
T_m	-	matrix temperature	k
F	-	friction factor	
C_v	-	gas heat capacity	$J/kg \cdot K$
c_m	-	matrix heat capacity	$J/kg \cdot K$
ϕ	-	porosity	
R_c	-	gas constant	$J/kg \cdot K$
γ	-	ratio of specific heats	
L	-	length of regenerator	m
$a(t)$	-	left endpoint (piston position)	m
$b(t)$	-	right endpoint	m